A large-scale, in vivo transcription factor screen defines bivalent chromatin as a key property of regulatory factors mediating Drosophila wing development

Claus Schertel, Monica Albarca, Claudia Rockel-Bauer, et al.

Genome Res. published online January 7, 2015
Access the most recent version at doi:10.1101/gr.181305.114

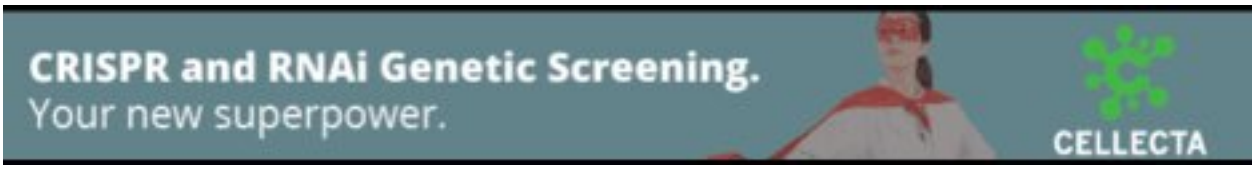

A large-scale, *in vivo* transcription factor screen defines bivalent chromatin as a key property of regulatory factors mediating *Drosophila* wing development

Claus Schertel[1,*], Monica Albarca[2,*], Claudia Rockel-Bauer[1], Nicholas W. Kelley[3], Johannes Bischof[1], Korneel Hens[2, 4], Erik van Nimwegen[3,**], Konrad Basler[1,**], Bart Deplancke[2,**]

*equal contribution

**corresponding authors

Affiliations:

[1]Institute of Molecular Life Sciences, University of Zurich, Switzerland

[2]Laboratory of Systems Biology and Genetics, Institute of Bioengineering, School of Life
Sciences, Ecole Polytechnique Fédérale de Lausanne and Swiss Institute of Bioinformatics, Lausanne, Switzerland

[3]Biozentrum, University of Basel and Swiss Institute of Bioinformatics, Basel, Switzerland

[4]current address: Centre for Neural Circuits and Behavior, University of Oxford, United Kingdom

Correspondence: erik.vannimwegen@unibas.ch

konrad.basler@imls.uzh.ch

bart.deplancke@epfl.ch

Running Title: Bivalently marked TFs regulate wing development

Key words: Drosophila / transcription factor / chromatin / bivalent histone marks

Abstract

Transcription factors (TF) are key regulators of cell fate. The estimated 755 genes that encode DNA binding domain-containing proteins comprise about 5% of all *Drosophila* genes. However, the majority has remained uncharacterized so far due to the lack of proper genetic tools. We generated 594 site-directed transgenic *Drosophila* lines that contain integrations of individual *UAS-TF* constructs to facilitate spatio-temporally controlled misexpression *in vivo*. All transgenes were expressed in the developing wing and two thirds induced specific phenotypic defects. *In vivo* knock-down of the same genes yielded a phenotype for 50%, with both methods indicating a great potential for misexpression to characterize novel functions in wing growth, patterning and development. Thus, our UAS-TF library provides an important addition to the genetic toolbox of *Drosophila* research, enabling the identification of several novel wing development-related TFs. In parallel, we established the chromatin landscape of wing imaginal discs by ChIP-seq analyses of five chromatin marks and RNA pol II. Subsequent clustering revealed six distinct chromatin states with two clusters showing enrichment for both active and repressive marks. TFs that carry such `bivalent' chromatin are highly enriched for causing misexpression phenotypes in the wing, and analysis of existing expression data shows that these TFs tend to be differentially expressed across the wing disc. Thus, bivalently marked chromatin can be used as a marker for spatially regulated TFs that are functionally relevant in a developing tissue.

Introduction

Transcriptional regulation plays a pivotal role during the development of all living organisms. The ability of a cell to grow, differentiate, or respond to environmental cues requires the coordinated and regulated expression of hundreds of genes, which is mostly controlled by sequence-specific transcription factors (TFs) that act as activators or repressors (e.g. Davidson, 2006; Deplancke, 2009). Despite their importance for the development and life of organisms, the biological function of the majority of eukaryotic TFs remain poorly characterized. Since the human genome encodes approximately 1500 TFs and features abundant inherent functional redundancy (Tupler et al., 2001), it is desirable to study TFs in a model system that is genetically more tractable. The fruit fly *Drosophila melanogaster* provides powerful tools to study developmental gene regulatory networks: (i) The *Drosophila* genome is fully sequenced, annotated with high quality and genetically much more accessible than many mammalian genomes, which is important for mapping regulatory elements and inferring their activities (Arnold et al., 2013; The modENCODE Consortium et al., 2010; Nègre et al., 2011). (ii) The *Drosophila* wing constitutes a complex organ system that allows precise spatio-temporal genetic manipulation with the possibility to isolate large quantities of organ-specific biological material. (iii) 755 genes have been identified in *Drosophila* that contain a DNA binding domain (Adryan and Teichmann, 2006; Hens et al., 2011). This lower complexity makes it possible to comprehensively study all TFs in parallel *in vivo*, as illustrated by the detailed study of their developmental expression patterns using *in situ* hybridization (Hammonds et al., 2013). (iv) Open-reading frames (ORFs) have been cloned for the large majority of TF genes (Hens et al., 2011).

Studying gene function often relies on loss-of-function approaches. However,

about 75% of all *Drosophila* genes appear to be phenotypically silent upon loss-of-function (Miklos and Rubin, 1996). As such, mis- or overexpression provides a powerful alternative to study gene function in such cases. In addition, UAS-driven transgenes facilitate precise spatio-temporal control of gene expression (Brand and Perrimon, 1993). Moreover, the expressed transgene is exactly defined by the integrated DNA sequence. Thus, phenotypic effects are caused by the transgene alone and not by unspecific side effects. Finally, the introduction of a small protein tag (3xHA) provides the opportunity for biochemical applications while not having to rely on antibodies against the endogenous protein, making the transgenic animals an *in vivo* resource for studying all TFs.

Here, we report the generation and initial characterization of transgenic flies for the vast majority of *Drosophila* TFs. We also established the chromatin landscape of the developing wing disc by genome-wide profiling of five different chromatin marks as well as RNA pol II. The latter analyses revealed genes with simultaneous combinations of activating and repressing marks, also termed “bivalently” marked genes (Bernstein et al., 2006). Interestingly, we found that such genes were highly enriched for TFs with differential expression across the wing disc that also caused severe phenotypes in the wing upon misexpression. Our work therefore provides new insights into the biological relevance of chromatin bivalency in a developing organ.

Results

Library generation and phenotypic analysis

We generated a site-directed library of 594 *UAS-TF* lines by using the phiC31 integrase system and the landing site 86Fb on the third chromosome (for detailed information on the landing site, see Bischof et al., 2007). All transgenes are fused to a

3xHA-tag to facilitate biochemical applications. Importantly, anti-HA staining revealed correct subcellular localization of misexpressed TFs in the nucleus and experimental analyses on a select number of TFs showed the expected molecular behavior (**Supplemental Fig. S1A-C**), underscoring the quality of this TF resource.

We started to characterize the obtained transgenic lines by expressing all transgenes in the developing wing using *MS1096-Gal4* and recorded the induced phenotypes in the adult wing (see **Supplemental Table S1** for a complete list of all available transgenic lines and the corresponding phenotypes). *MS1096-Gal4* is ubiquitously expressed throughout the L3 larval stage within the wing pouch (**Supplemental Fig. S1D-F**) with stronger expression in the dorsal compartment (Capdevila and Guerrero, 1994; Lunde et al., 1998). We found that almost two thirds of all TFs (65.2%) are capable of inducing highly reproducible visible phenotypes in the wing upon expression by the *MS1096-Gal4* driver. These phenotypes include strong reduction of wing size (class ++: 76/594; 12.8%) or almost complete absence of the adult wing (class +++: 112/594; 18.9%). We also observed lethality for a large number of induced TFs (131/594; 22.1%) (**Fig. 1**). This lethality most likely stems from additional weak *MS1096-Gal4* activity in the wing hinge region (Neumann and Cohen, 1996 and **Supplemental Fig. S1D-F**) and during embryonic development (Marquez et al., 2001). However, when TFs of the lethal class were retested at lower temperature (18° C instead of 25° C), almost all crosses produced viable offspring that showed a strong phenotype (class +++, **Supplemental Table S1**). Since the lower temperature results in lower expression levels, this indicates that the phenotypic outcome of TF misexpression is dose-dependent. The fact that phenotypes were generally stronger in male offspring compared to their female siblings supports this hypothesis, because the *MS1096-Gal4* driver is located on the X-chromosome, thus

causing experimental males to be hemizygous while females are heterozygous for the driver transgene (**Supplemental Table S1**).

We further compared the abundance of phenotypes to an *UAS-ORF* library that mostly encodes non-TF proteins that were previously implicated in cell cycle control (Björklund et al., 2006; Schertel et al., 2013). After removing 34 TFs from the *UAS-ORF* data set to eliminate bias caused by this overlap, we found that induced TF expression results in significantly more and relatively stronger phenotypes in the wing compared to the set of *UAS-ORF* transgenes (p = 6.3e-10, Fisher's exact test)(**Fig. 1** and **Table 1**). Another class of genes that regulate gene expression involves microRNAs (miRNAs). These non-coding RNAs typically cause only modest gene expression changes of their targets (Selbach et al., 2008) and are thought to either fine-tune genes expression levels, or aid in ensuring expression robustness (Posadas and Carthew, 2014). In contrast, TFs can often act in a "switch-like" manner. Consistent with this general view, we found a significantly larger proportion of TFs that induce clearly visible phenotypes than miRNAs (p = 1.1e-10, Fisher's exact test) (**Table 1**). Next, we extracted all 511 genes that are annotated under the term "wing disc development" in FlyBase among which 72 were tested in our study. We found a significantly greater proportion of phenotypes among these 72 TFs compared to the remaining 522 in our library (p = 0.02, Fisher's exact test), further underscoring our hypothesis that we can identify important wing disc factors via misexpression. Finally, we explored whether the probability of inducing a misexpression phenotype is inversely related to the endogenous expression level of the respective TF. The underlying reasoning is that additional expression from a transgene may cause a more benign effect when the focal gene is already highly expressed compared to a low expression state. To test this hypothesis, we employed RNA pol II ChIP-seq data that

were generated as part of our aim to characterize the chromatin landscape of the imaginal wing disc (see below). TFs were grouped into five bins based on RNA pol II occupancy, with each bin containing 20% of all TFs. We found that significantly more and stronger phenotypes are caused by TFs whose endogenous transcription in wing disc is low compared to TFs whose endogenous transcription is already high, reflecting an important disruption of the endogenous wing gene regulatory network by the ectopically expressed TF (**Fig. 2A**)(e.g. p = 1.5e-5 for a greater proportion of severe (++, +++, lethal) phenotypes in the lowest 20% compared to the highest 20%, Fisher's exact test). The same analysis based on RNAi phenotypes revealed the opposite trend, although less significant (p = 0.037, Fisher's exact test): genes that are endogenously higher expressed are slightly more prone to cause phenotypic effects upon knock-down than more lowly expressed genes (**Supplemental Fig. S2A**).

In summary, our analysis strongly suggests that our TFs transgenes were successfully induced in wing disc and produced functional proteins. Furthermore, a high proportion of the transgenic TFs can induce specific phenotypes upon misexpression, providing a valuable resource to study the molecular function of TFs.

Comparison of OE and RNAi phenotypes

Next, we compared TF misexpression to TF knock-down by *in vivo* RNAi (Dietzl et al., 2007). We randomly chose RNAi lines from the VDRC *in vivo* collection. We preferred the site-directed KK lines that were predicted to cause no off-target effects. We found that about half (52.7%) of the TFs that we knocked-down by *UAS-RNAi* lines (n=237) caused a phenotypic effect in the wing (**Table 1**) closely resembling the ratios found in other studies (Molnar et al., 2012).

Upon comparing misexpression and knock-down phenotypes, we first focused on TFs that have only a CG number assigned to them and have thus so far been poorly characterized. The fact that no specific role has been defined in previous studies for these TFs could indicate that they target only a small set of genes or that they only act in very specific conditions. However, we found a large number of phenotypes caused by misexpression of these uncharacterized TFs (**Fig. 2B**). Although the proportion (91/195, 46.7%) is much lower than the corresponding proportion of TFs that have an assigned name (296/399, 74.2%), it nevertheless suggests that many TFs remain to be characterized that are functionally relevant during wing development (**Fig. 2B**). The same analysis performed on RNAi-mediated knock-down phenotypes showed little difference between the proportion of different phenotypes for characterized and uncharacterized TFs.

We subsequently compared the qualitative effects that were caused by individual TFs upon misexpression or RNAi, respectively. We found a relatively weak correlation between phenotypes caused by elevated and reduced TF levels. Roughly half (90/179, 50.3%) of all TFs that caused phenotypes upon misexpression also caused phenotypes upon knock-down. Surprisingly, this proportion is also reached for the class that did not induce phenotypes upon misexpression (**Supplemental Fig. S2B, C**). Here, 16 out of 30 (53.3%) did induce a phenotype when knocked-down. However, there is only little correlation between the RNAi and misexpression phenotypes indicating that misexpression can provide additional information that would be missed by RNAi knock-down alone. Of the 91 “novel” TFs that caused misexpression phenotypes, 57 were also tested by RNAi. Of these, 29 caused a wing phenotype upon knock-down suggesting that those genes are important during wing development (**Supplemental Table S1**). In addition, we identified 4

uncharacterized TFs (*CG10431*, *CG10565*, *CG10654* and *CG11398*) that caused a phenotype upon knock-down but not by misexpression.

In summary, we found 97 phenotypes for previously uncharacterized TFs either by RNAi, by misexpression, or both. In general terms however, misexpression phenotypes were more abundant supporting our hypothesis that misexpression is a powerful method to study specific gene functions that might not be accessible to loss-of-function approaches.

The chromatin landscape of the wing disc and its relationship to misexpression phenotypes

Chromatin profiling has proven to be a valuable strategy to infer novel regulatory principles (The modENCODE Consortium et al., 2010), making it a complementary strategy to TF misexpression and knockdown approaches. To determine the chromatin landscape in the wing disc, we used ChIP-seq to map enrichment of histone modifications in imaginal wing discs at 120 h of development. In addition, we performed RNA pol II ChIP-seq as a proxy for transcriptional activity, which we aimed to relate to the chromatin state. We noted however a good correlation between published wing gene expression data (McKay and Lieb, 2013) and RNA pol II gene promoter and gene body DNA occupancy (**Fig. 3A**, **Supplemental Fig. S3A**). To cover multiple active chromatin states, we used two antibodies that simultaneously recognize more than one histone modification: (i) an antibody against H3K4me2 and H3K4me3 that we named H3K4me2-3 and (ii) one that recognizes H3K79-mono, -double and -triple methylation, referred to as H3K79me1-2-3. All other antibodies specifically recognize individual histone modifications (H3K27ac, H3K4me1, and H3K27me3). A correlation heat map of the resulting histone modification enrichment

profiles validated our data sets, since, as expected, activating marks grouped closely together (**Supplemental Fig. S3B**).

Subsequent clustering of the resulting chromatin profiles along gene bodies as well as the proximal regions 2000 bp up- and downstream of the respective genes using seqMINER (Ye et al., 2011) revealed six distinct groups with quantitatively comparable enrichment for certain histone modifications and RNA pol II on genes within each group (**Fig. 3A**). Clusters 1-3 contain genes with strong to moderate RNA pol II DNA occupancy, as well as enrichment for histone modifications that are characteristic of active transcription (H3K4me2-3, H3K27ac, H3K79me1-2-3 and the enhancer mark H3K4me1, **Supplemental Fig. S4**). We thereby note that even though H3K4me1 has the appearance in **Fig. 3A** of covering the entire gene body, we found it specifically enriched in introns and 5'upstream gene regions, as expected (**Supplemental Fig. S5A, B**). A Gene Ontology enrichment analysis further revealed that clusters 1-3 tend to contain constitutively active genes involved in rather generic molecular processes annotated under very general GO terms (see **Supplemental Table S3** for a complete list of all GO enrichments for each cluster).

Cluster 4 contains transcriptionally active genes given the high RNA pol II DNA occupancy and enrichment for the H3K79me1-2-3 and H3K4me2-3 marks, even though these genes display relatively low H3K27ac levels. Surprisingly, we found that a subset of 241 genes in cluster 4 (**Supplemental Table S2**) are also enriched for the repressive mark H3K27me3 (subsequently named cluster 4b, Methods). This suggests that these genes are repressed in parts of the wing disc, and expressed in others. Alternatively, it could reflect a bivalent chromatin state, which has been observed at developmentally relevant genes in mammalian cells (Bernstein et al., 2006), but which has to our knowledge not been previously described in

Drosophila. Interestingly, when only cluster 4b genes were taken into account, the strongest GO term enrichment was found for “organ development” or even more specifically “imaginal disc development” indicating that the bivalent chromatin state of these genes may be reflective of their regulatory potential during wing development (**Table 2**). Cluster 5 contains genes with relatively low RNA pol II occupancy, except around their transcription start sites (TSSs). This could mean that the activity of these genes is heterogeneous across the wing disc with them being transcribed in only a small subsection of the wing disc. Alternatively, it may indicate that many of these cluster 5 genes are in a transcriptionally poised state (Muse et al., 2007; Zeitlinger et al., 2007) (**Fig. 3B**). This is consistent with the generally low levels of the H3K79me1,2,3 transcriptional activity mark on these genes. Moreover, genes within this cluster tend to be associated with gene-proximal or intronic elements that are only enriched for H3K27me3 and H3K4me1 (**Fig. 3B**). This is similar to the enrichment profile observed for group 4b genes, except that genes in cluster 5 appear not to be transcribed. This particular combination of H3K4me1 and H2K27me3 marks has first been observed in human embryonic stem cells (hESCs) where it was revealed to annotate “poised” enhancers that mediate state- or cell type-specific expression of developmental genes (Bajpai et al., 2010; Shlyueva et al., 2014). Consequently, such poised enhancers were found to be associated with lowly transcribed genes, consistent with the relatively low transcriptional activity of genes belonging to cluster 5. For consistency, we also grouped the 194 genes that exhibited such H3K27me3 enrichment in a subcluster (5b as opposed to genes without H3K27me3 enrichment which were grouped in subcluster 5a). Interestingly, cluster 5b is enriched for genes that are involved in transcriptional regulation such as TFs (**Tables 2** and **3**) as reflected by the GO enrichment for “regulation of RNA

biosynthetic process". Finally, cluster 6 contains around 7000 genes without enrichment for any of the probed histone modification marks consistent with the fact that these genes also exhibited very low or undetectable RNA pol II activity. For some genes in cluster 6, we observed an enrichment of RNA pol II at the 3'end, but further investigation showed that this RNA pol II signal corresponds to actively transcribed adjacent genes.

To validate our clustering results, we applied the same analytical approach on published H3K4me1, H3K4me1, H3K27ac, H3K27me3, and RNA pol II data sets from S2 cells and observed in general a good, qualitative agreement with our wing disc data in terms of cluster type and gene composition (**Supplemental Fig. S6A, B**) (Kharchenko et al., 2011). In addition, we determined the overlap with previously defined chromatin states (Filion et al., 2010) by calculating the percentage of genes in each cluster covered by each of the "chromatin colors". The resulting data (discussed in **Supplementary Figure S6C**) are in line with expectations, further validating our clustering approach. For example, clusters 4 and 5 contain the highest number of "blue" (Polycomb)-labeled genes with a further distinction between the subclusters with or without "H3K27me3" in that a greater proportion of blue was observed in the "with" subclusters, consistent with the involvement of Polycomb in establishing this repressive mark (Cao et al., 2002; Czermin et al., 2002).

Next, we asked if a particular chromatin state is enriched for functionally relevant TFs as measured by the capability to induce phenotypes upon (mis)expression. Clusters 1, 2 and 3, which represent constitutively and highly transcribed ("housekeeping") genes, are depleted for such TFs. Furthermore, the few TFs that are contained within these clusters do not induce strong phenotypes upon misexpression in the wing. In contrast, we observed a strong relationship between

phenotypic strength and the bivalent nature of the chromatin state surrounding the TF-coding genes in that both clusters 4b and 5b are strongly enriched for TFs that induced strong wing phenotypes or even lethality (**Table 2**). These data suggest that genes that are associated with bivalently labeled genomic elements tend to be functionally relevant for wing development (**Fig. 4**).

Finally, we compared our wing disc-specific chromatin mark ChIP-seq data to similar data published by the modENCODE Consortium using entire larvae (Oregon strain) but also at the third instar stage (Nègre et al., 2011). We specifically observed clear histone modification enrichment differences in several chromosomal regions containing bivalently marked genes (e.g. *ara* and *caup*, **Supplemental Fig. S7A**) that are expressed in the wing disc or in regions containing genes that are repressed in the wing (e.g. *Ubx-abd-A* cluster, **Supplemental Fig. S7B**). For example, compared to the modENCODE Consortium data, we found a greater enrichment of activating marks for bivalent, but actively transcribed genes of cluster 4b (**Supplemental Figs. S7A, C, and D**). In contrast, we found that these activating marks are virtually absent from regions containing repressed wing genes, whereas this is not the case in the modENCODE Consortium data (**Supplemental Fig. S7B**), implying signal contribution from other imaginal disc types. These observations re-emphasize the functional importance of bivalently marked genes given that they appear to be transcriptionally controlled in an intricate wing disc-specific manner.

Cell autonomy of bivalent marks

The observation of bivalently marked chromatin may stem from two intriguing scenarios. These bivalent marks (activating and repressing) could be present cell-autonomously, i.e. within individual cells on individual genes. Alternatively, the

different marks could be derived from separate cell populations within the disc. In this scenario, a specific gene would be expressed in a cluster of wing disc cells and therefore display activating marks, while it is repressed in other cells of the disc and would display repressive marks in these cells. Since the ChIPed material was isolated from entire discs, the resulting pattern would show activating and repressing marks as an average over the entire cell population. Given that H3K27me3 enrichment and transcriptional elongation (as evidenced by the enrichment of RNA pol II in gene bodies of cluster 4) are considered incompatible (Schmitges et al., 2011; Voigt et al., 2013), the presence of heterogeneous cell populations within the disc appears the most likely scenario. To validate this hypothesis, we used three microarray expression data sets that were collected from wing disc samples. The first data set contains genes that showed at least a two-fold enrichment in either the body wall or the hinge and wing blade region (BW/WB) of the disc (Butler et al., 2003). The other two data sets were collected by microarray expression analysis of anterior and posterior (A/P) wing disc cells in our own laboratory (Simigdala, unpublished data) or by others (Ibrahim et al., 2013). Of all genes in clusters 4b and 5b combined, 12.4% (54/435) showed a compartmentally restricted expression pattern, which is about five-fold higher than for all remaining genes (2.6%, 373/14505) (**Table 3**). The effect is even more pronounced for bivalently labeled TFs, where the enrichment in clusters 4b and 5b is ten-fold greater (25% (40/160) versus 2.4% (14/595)). This strongly suggests that the bivalent marks for these genes derive from distinct expression domains within the wing disc. However, there are also a large number of bivalently marked genes that are not expressed in a spatially restricted way. These genes may either have expression patterns in subsets of wing disc cells that were not captured by the available data sets or carry both marks in a cell-autonomous fashion. Irrespective of the cell autonomy

of these marks, our data suggests that bivalent chromatin is a hallmark of genes that are highly relevant for wing development.

Discussion

TF library and phenotypic analysis

We present an *in vivo* resource to systematically study TF function by misexpression in *Drosophila*. The number of phenotypes and the strength of the observed phenotypes are significantly greater than for previously analyzed gene sets that did not include TFs. This is not surprising since TFs typically regulate many target genes, and the number of genes targeted in a particular condition is strongly dependent on the nuclear abundance of the TF (Biggin, 2011; Simicevic et al., 2013). Thus, the induction of a particular TF likely significantly affects its DNA binding and gene regulatory activity, resulting in the subsequent misexpression of dozens or even hundreds of genes.

A comparison with other large-scale datasets provided several important molecular insights. For example, we observed a bias in the capability of phenotype induction by misexpression of TFs toward those that are lowly transcribed in the wing disc. This implies that elevating the abundance of already highly expressed TFs tends to have little impact. There are exceptions to this rule however, suggesting that the occupancy of these specific TFs on target DNA binding sites may not be saturated under physiological conditions. This view is consistent with the notion that accessible DNA sites compete with one another for TF binding, resulting in increased binding upon increasing TF levels (Janssen et al., 2000; Simicevic et al., 2013). TF misexpression may thus allow a comprehensive characterization of the genome-wide DNA binding potential of TFs. Another insight is the relatively low correlation

between knock-down and misexpression phenotypes. Underlying reasons may include i) misexpression-related activating or inhibiting effects such as dominant-negative phenotypes, ii) the disruption of a multimeric protein complex or changing the abundance of interacting proteins (Prelich, 2012), iii) loss-of-function effects caused by the C-terminal HA-tag (Bischof et al., 2013), and iv) RNAi-related artifacts such as off-target effects or non-functional RNAi constructs, which for the Vienna RNAi lines has been estimated to mount up to 40% (Dietzl et al., 2007). Misexpression-only phenotypes could additionally be due to the low endogenous expression of the respective TF in the wing (this is true for at least 7 TFs according to our RNA pol II data) or redundant activity with other TFs. One example for the latter involves *dl* and *Dif*, two NFkB homologs that cause lethality upon misexpression but fail to induce a knock-down phenotype and have an established redundant role in immunity (Matova and Anderson, 2006). Nevertheless, TFs that show both misexpression and knock-down phenotypes are likely of highest biological interest. We found 25 such TFs that have never been characterized before and are currently only annotated by a CG number (**Supplemental Table S1**). Thus, these genes represent interesting candidates with potentially important roles in wing development.

In summary, our analysis provides an initial phenotypic characterization of 594 *Drosophila* TFs. We identified many TFs that induce highly specific phenotypes in the wing. The observed effects are quantitatively and qualitatively more pronounced than RNAi-mediated knock-down, indicating that misexpression is a powerful alternative to characterize gene function.

Functional relevance of bivalently marked genes

Our histone modification ChIP-seq analyses revealed many genes that display both activating and repressive chromatin marks. Our data suggests that at least some

of these bivalent states derive from spatially separated expression domains within the wing disc. The underlying chromatin regions are therefore not bivalent *sensu stricto*. Genes whose expression is restricted to certain areas but do not appear to have bivalent marks might be regulated by different mechanisms, e.g. by region-specific transcriptional activators or repressors (Davidson and Levine, 2008). Conversely, for a number of genes that display bivalent marks, there is no evidence that they are expressed in the wing disc in spatially distinct fashion. It therefore cannot be excluded that these genes may carry genuine bivalent marks within individual cells similar to those genes that were identified in distinct mouse and human cell lines using sequential ChIP-seq experiments (Voigt et al., 2012). The fact that we also observed bivalent gene clusters in S2 cells may lend credibility to the latter hypothesis, but since S2 cells are non-clonal (Schneider, 1972), it is also possible that such bivalency stems from cell population heterogeneity. However, additional in-depth experiments will be required to unequivocally establish the existence of bivalent chromatin in *Drosophila*.

We also found many genes that are enriched for both H3K4me1 and H3K27me3 across their genomic loci. Such a chromatin signature was, as already indicated, first discovered in human ESCs and subsequently confirmed in mouse ESCs (Bajpai et al., 2010; Zentner et al., 2011). Since such bivalently marked regions were mostly found at distal loci of genes that are inactive in ESCs, but become transcribed during ESC differentiation, these regions are thought to correspond to poised enhancers. In *Drosophila*, such bivalently marked enhancers were recently found in the developing mesoderm (Bonn et al., 2012), yet their transcriptional importance in this tissue is unclear as these enhancers were found to be mostly repressed instead of poised. Thus, similar to bivalent chromatin on genes, the

functional relevance of bivalent chromatin on enhancers remains poorly understood. An important outcome of our study in this regard is that chromatin bivalency constitutes an interesting and novel criterion next to more obvious measures such as high, system-specific, or developmentally dynamic expression to identify genes that may have a key role in tissue development. Three lines of evidence support this claim for wing development: (i) bivalently marked genes are enriched for the GO term “imaginal disc development”, (ii) TFs cause significantly more and stronger phenotypes when encoded by bivalently compared to non-bivalently marked genes, and (iii) many genes and especially TF-coding ones that display bivalent marks show spatially restricted expression in the wing disc indicating functional relevance during development. Thus, our data support the notion that bivalent chromatin is a hallmark of TF-coding genes with important regulatory roles in a developing organ such as the wing, thereby providing novel insights into the biology of its development.

Methods

Transgene cloning and transgenesis

A detailed description of the transgene production can be found in (Bischof et al., 2013). Expression plasmids were generated from our own TF open-reading frame (ORF) collection by Gateway cloning (Hens et al., 2011). Subsequently, UAS-TF expression plasmids were pooled, injected and the progeny was clonally crossed to balancer lines to establish individual stocks. Transgenes were identified by Sanger sequencing of the respective barcode in standardized PCRs. All transgenic lines created in this study are publicly available through our website (www.flyorf.ch).

Tester strain for ChIP-seq and RNA-seq

A *spalt major* (*salm*) enhancer fragment (4.8 kb from pLB4-1, our own unpublished data, a brief description can be found in FlyBase: FBrf0211371) was digested with EcoRI, introduced in pEGFP.attB (Bischof et al., 2013), and tested for correct orientation. The resulting construct was injected into strain ΦX-86Fb and a homozygous *salm^{E}-eGFP* strain was established. The transgene *salm^{E}-eGFP* was subsequently recombined with *C765-Gal4*, *Gal80^{ts}*, both present on the 3rd chromosome.

Mass isolation of wing discs

Virgins of *yw;; C765-Gal4 tubGal80^{ts} salm^{E}-eGFP* were crossed to the UAS-TF strains and kept at 21˚ C for 7 days. Larvae were shifted to 29˚ C 13 h prior to harvest. 5 ml of wandering L3 larvae were used for mass isolation of wing discs. We adapted a recently published protocol (Marty et al., 2014). 5 ml of larvae were disrupted using the gentleMACS dissociator (Milteny). The disrupted material was crosslinked in 1 %

formaldehyde for 10 min at room temperature. Crosslinking was stopped and formaldehyde quenched with 125 mM glycine for 5 min and washed two times in PBS (PBS Dulbecco, L 182-50, Biochrom AG). The material was separated by a gradient of 10 % Ficoll (Ficoll PM 400, 17 0300 50, GE Healthcare) as the upper phase, 20 % Ficoll as the middle phase and 30 % Ficoll as the lower phase. The duration of the gradient centrifugation was 20 min at 5000 rpm. The discs were enriched at the interphase between 10 % and 20 %. Imaginal discs were washed once with PBS to clean them from residual Ficoll. All Ficoll solutions were made with PBS.

Sorting of wing discs (Bio Sorter)

Mass-isolated wing discs were sorted from the rest of the organs by using criteria for the density and the fluorescence intensity of the wing disc (BioSorter, Union Biometrica). Wing discs were sorted based on fluorescence intensity (1500 – 30000 green peak hight) and counter-sorted according to autofluorescence. Green PMT voltage was set to 450, sort delay to 25 (mS) and drop width to 10 (mS). The sorting mode was set to enrichment, and the wing disc recovery rate was typically 90 % of the input material. Residual contaminants were manually removed from the sample. Discs were frozen in batches of 1000 discs. Usually, mass isolation of 5 ml of larvae yielded 1000 to 1500 discs.

ChIP-seq and library preparation

The ChIP protocol was adapted from Weinmann and Farnham (Weinmann and Farnham, 2002). Briefly: Crosslinking was performed during the mass isolation (see mass isolation). Wing discs were resuspended in cell lysis buffer (5 mM PIPES ph

8.0, 85 mM KCl, 0.5 % NP-40, protease inhibitors), snap frozen in liquid nitrogen and kept at -80˚ C. Prior to ChIP wing discs were thawed on ice, cell lysis buffer was removed, the discs were resuspended in 200 µl nuclear lysis buffer (50 mM Tris-Cl, pH 8.1, 10 mM EDTA, 1 % SDS, protease inhibitors), and transferred into two sonication vials (microTUBE, 520045, Covaris). The chromatin was fragmented using the Covaris S220 (duty cycle: 10 %; intensity: 5; cycles/burst: 200, time: 40 sec) to an average size of 500 bp. Afterwards 200 µl were pooled, insoluble material was removed by centrifugation, and soluble chromatin extract was used for IP. 200 µl IP dilution buffer (0.01 % SDS, 1.1 % Triton X-100, 1.2 mM EDTA, 16.7 mM Tris-Cl pH 8.1, 167 mM NaCl, protease inhibitors) and the indicated antibodies were added to the chromatin and incubated over night at 4˚ C. IP was performed by adding 60 µl magnetic beads (MagnaChIP^{TM} Protein A and G, 16-663, Millipore) washed once in nuclear lysis buffer : IP dilution buffer (1 : 1) (Nu : IP), to the chromatin. The mix was incubated for 2 h on a rotating wheel. Samples were washed 4 times for 3 min using 1 ml of IP wash buffer (100 mM Tris-Cl pH 8.0, 500 mM LiCl, 1 % NP40, 1 % deoxycholic acid, protease inhibitors). For elution and reversal crosslink, the beads were resuspended in 50 µl of Nu : IP containing 20 µg RNAse A, and incubated at 65˚ C for at least 4 h. Following, 40 µg Proteinase K was added and samples were kept at 45˚ C for 2 h. DNA was purified using the MinElute PCR purification kit (28004, Qiagen). DNA was eluted in 24 µl H_2O. Concentration was measured from 4 µl by Qubit using the dsDNA HS assy kit. Libraries were prepared using the Illumina TruSeq ChIP Sample Prep Kit (IP-202-1012, Illumina). Libraries were sequenced on an Ilumina HiSeq 2500 machine at the Lausanne Genomics Technologies Facility (GTF), obtaining more than 200 million 100 bp reads per sequenced lane.

The following antibodies (Abcam Inc., Cambridge, USA) were used in this study: ab6002: anti-Histone H3 (tri methyl K27); ab28940: anti-Histone H3 (mono+di+tri methyl K79); ab8895: anti-Histone H3 (mono methyl K4); ab6000: anti-Histone H3 (di+tri methyl K4); ab4729: anti-Histone H3 (acetyl K27) antibody; a mix of ab5408 (phospho S5 antibody 4H8) and ab817 (antibody 8WG16): anti RNA-polymerase II-CTD repeat YSPTSPS of Pol II largest subunit (RPB1); ab9110: anti-HA (used for Pangolin ChIP).

qRT-PCR

Flies carrying the transgenic TF of interest were crossed to *yw;C765-Gal4 tubGal80ts salm-eGFP/TM6b*. Flies were kept at 21˚C until 24 hours before dissection when they were shifted to 29˚C to induce transgene expression. RNA was isolated of 2 x 30 - 40 wing discs and purified using the RNA XS kit (NucleoSpin® RNA XS, 740902.10, Machery-Nagel). 500ng of RNA were reverse transcribed into cDNA according to manufacturers guidelines (First Strand cDNA Synthesis Kit for RT-PCR, 11483188001, Roche) using Oligo-p(dT)15 Primer. cDNA was directly used as template for qRT-PCR using the ABI SYBR green system. Transcript levels were normalized to act, tub and Tbp.

The following gene specific primer sequences were used:

Tub for: GCCAGATGCCGTCTGACAA

Tub rev: AGTCTCGCTGAAGAAGGTGTTGA

Act for: GCCCATCTACGAGGGTTATGC

Act rev: AATCGCGACCAGCCAGATC

TBP for: CGCGCATCATCCAAAAGC

TBP rev: GCCGACCATGTTTTGAATCTTAA

Hid for: TCTACGAGTGGGTCAGGATGT

Hid rev: GCGGATACTGGAAGATTTGC

Rpr for: TCGATTTCTACTGCAGTCAAGG

Rpr rev: GAGTAAACTAAAATTGGGTGGGTGT

Omb for: GCGAAGGGCTTTCGTGATAC

Omb rev: GACCCTCGGTTCGACATCAG

Data analysis

Peak calling

Bowtie 2 (version 2.0.0-beta6) (Langmead and Salzberg, 2012) was used to align the sequencing reads using default parameters. The BDGP5.66 Drosophila genome annotation version was used as reference. The program makeUCSCfile from HOMER (Heinz et al., 2010) was used to produce visualization files in bedGraph format. BedGraph files were normalized to 10 million tags (HOMER default parameters). The program findPeaks from the HOMER package was used to identify regions enriched for histone modification marks, and data from a H3 ChIP-seq experiment was used as a control. RNA pol II ChIP was analyzed using HOMER and findPeaks, and tags from total input DNA sample were used as control. The findPeaks option called region was set to 500 bp for all the histone modification marks and RNA pol II, except for H3K27me3, for which the region was set to 5000 bp. To determine the distribution of chromatin marks near the TSS, the program annotatePeaks (HOMER) in hist mode was used and the average tag coverage 1000 bp upstream and downstream of the TSS was calculated using a resolution of 10 bp.

Gene cluster analysis

Clustering of chromatin marks and RNA pol II profiles was performed using seqMINER (Ye et al., 2011). The gene profile analysis covered the gene body and 2000 bp upstream and downstream with the latter regions being considered gene-proximal. Gene body sizes were normalized and divided in 100 bins and the upstream and downstream parts were divided in 20 bins each. The k-means ranked method was used to find the clusters. The number of clusters was set to 8 (k=8). seqMINER produced 8 clusters, 3 of which did not show enrichment for any of the chromatin marks. These 3 clusters were joined to form cluster 6. To identify genes specially enriched for H3K27me3 in clusters 4 and 5, we first selected the H3K27me3-enriched regions obtained using HOMER after which we explored the overlap of H3K27me3-enriched regions with genes in cluster 4 and 5. The genes whose TSS overlapped these H3K27me3-enriched regions were finally grouped separately in clusters 4b and 5b respectively.

Chromatin mark and RNA pol II correlation analysis

To generate the heat map representing the linear Pearson correlation among tag densities of chromatin marks and RNA pol II, regions enriched for chromatin marks or for RNA pol II were split into 100 bp bins after which the number of tags in each bin was calculated using HOMER. Chromatin mark tag density was normalized using H3 and RNA pol II tag density with an input DNA sample. The Pearson linear correlation was then calculated among log2 ratio enrichment profiles for all pairs of chromatin marks and RNA pol II (one pseudo tag was added to avoid zero values).

RNA pol II and RNA-seq correlation analysis

To determine the extent of correlation between the RNA pol II ChIP-seq and RNA-seq data, the RNA pol II ChIP-seq tags at respectively the promoter (250 bp upstream

and 250 bp downstream from the transcription start site (TSS)), and along the gene body (250 bp downstream of the TSS to 250 bp upstream of the transcription end site (TES)) were counted using HOMER. Tag counts from a total DNA sequenced sample were used for normalization. RNA pol II and RNA-seq data were then transformed using log2 and quantile normalization (one pseudo tag was added to avoid zero values).

H3K4me1 genomic distribution analysis

The cis-regulatory element annotation system (CEAS) (Shin et al., 2009) was used to estimate the relative enrichment of H3K4me1 in each gene feature in relation to the whole genome. CEAS also provides a summary report showing a pie chart of how H3K4me1-enriched regions distribute over specific gene-related categories.

General statistics

Fisher's exact test, as implemented in R (R Development Core Team, 2006), was used to determine the significance of proportional differences in phenotype strength upon misexpression or knock-down for distinct functional categories.

Data Access

The ChIP-seq data from this study have been submitted to the NCBI Gene Expression Omnibus (GEO; http://www.ncbi.nlm.nih.gov/geo/) under accession number GSE59769. Accession numbers for the individual chromatin marks are as follows: GSM1446260 (H3K4me1), GSM1446261 (H3K4me2-3), GSM1446262 (H3K27me3), GSM1446263 (H3K27ac), GSM1446264 (H3K79me1-2-3), and for RNA pol II (GSM1446265).

Acknowledgements

The authors want to thank Edy Furger, Nellcia Wang and Jean-Daniel Feuz for technical assistance, the Lausanne Genomic Technologies Facility (GTF) and VITAL-IT for respectively sequencing and server support, and George Hausmann for critical reading and suggestions on the manuscript. This work was supported by a Sinergia grant (#CRSI33_127485) of the Swiss National Science Foundation and by Institutional Support by the Ecole Polytechnique Federale de Lausanne (EPFL).

Disclosure declaration

The authors declare no competing interests.

Figure Legends

Figure 1: Phenotypic analysis of the TF library by *MS1096-Gal4*-driven expression in the developing wing. Phenotypes upon misexpression by *MS1096-Gal4* (black bars) are compared to RNAi knock-down (grey bars) and two other misexpressed gene sets: cell cycle regulators (white bars) and miRNAs (green bars). Phenotypic strength was recorded from no effect, weak growth or patterning defects (+) to severe size or patterning defects (++), almost complete absence of wings (+++) to lethality (lethal) and bars show the distribution of observed phenotypes for each data set. Representative examples for the phenotypes (+ to +++) are shown. Arrowheads point to patterning defects.

Figure 2: Characteristics of phenotype-inducing TFs. (A) The misexpression phenotype distributions of TFs belonging to specific RNA pol II occupancy bins (from the lowest to the highest 20% RNA pol II occupancy) are compared. RNA pol II DNA occupancy was used here as a proxy for the extent of TF expression. Color-coding of the bars applies also to panel B. **(B)** Effects of overexpression are compared to those of RNAi-mediated knockdown. *UAS-TF* and *UAS-RNAi* were grouped into known genes with annotated names and uncharacterized genes that are only annotated by a CG number.

Figure 3: The chromatin landscape of wing discs at the third instar larval stage. (A) Clustering of all detected genes according to the distribution of five histone marks and RNA pol II as measured by ChIP-seq. Activating marks are indicated in green, repressive marks in red. The location of the transcription start (TSS) and the transcription end sites (TES) is indicated by lines within each histone modification

column. Previously published wing disc RNA-seq data (McKay and Lieb, 2013) is also presented to directly link histone modification, RNA pol II enrichment and gene expression. **(B)** Representative examples for genes in clusters 4a, 4b, 5a and 5b are shown ("a" reflects genes with low H3K27me3 enrichment, while genes in "b" reflect high enrichment of this mark). Gene loci are indicated at the bottom of the panels and the cluster number is listed at the top of the panels. The same molecular marks as in (A) are displayed. The scale for all tracks represents the tag depth per bp, except for the RNA-seq data for which the $\log_2$ of (FPKM+1) is plotted.

Figure 4: Distribution of phenotypes induced by TFs in the different clusters. The chart illustrates the distribution of phenotypes caused by misexpression of all TFs and from each cluster (c1-c6, X-Axis) by *MS1096-Gal4* in the wing.

Tables

Table 1: Comparison of phenotype abundance to other gene sets

Table 1 Proportion of wing phenotypes induced by different gene libraries

	lethal	+++	++	+	total phenotypes	no effect	total genes
UAS-TF	131	112	76	68	387	207	594
(%)	(22.1)	(18.9)	(12.8)	(11.4)	(65.2)	(34.8)	
UAS-ORF[1]	13	93	72	118	296	324	620
(%)	(2.1)	(15.0)	(11.6)	(19.0)	(47.7)	(52.3)	
UAS-miR[2]	14	5	8	41	68	111	179
(%)	(7.8)	(2.8)	(4.5)	(22.9)	(37.1)	(62.9)	
UAS-TF^{RNAi}	13	13	37	62	125	112	237
(%)	(5.5)	(5.5)	(15.6)	(26.2)	(52.7)	(47.3)	
"Wing disc" [3]	21	13	9	12	55	17	72
(%)	(29.2)	(18.1)	(12.5)	(16.7)	(76.4)	(23.6)	

[1] (Schertel et al., 2013): 34 TFs were removed from the data set for this analysis
[2] (Schertel et al., 2012)
[3] Subset of TFs that are present in our library and are defined by the search term "wing disc development" in FlyBase
All transgenes induced by *MS1096-Gal4*, numbers indicate absolute number of transgenes that induce the indicated phenotype, numbers in brackets indicate % of total number of transgenes tested

Table 2: Detailed information of chromatin cluster content

Table 2 Gene content of each chromatin cluster

Cluster	Genes	TFs (%)	TFs tested (%)	TFs causing misexpression phenotype (%)
1	1465	48 (3.2)	48 (100.0)	23 (47.9)
2	1823	131 (7.2)	116 (88.5)	48 (41.4)
3	1999	127 (6.4)	98 (77.2)	57 (58.2)
4a	939	46 (4.9)	37 (80.4)	23 (62.2)
4b	241	69 (28.6)	53 (76.8)	48 (90.6)
5a	842	24 (2.9)	18 (75.0)	14 (77.8)
5b	194	90 (46.4)	63 (70.0)	57 (90.5)
6	7434	168 (2.3)	145 (86.3)	104 (71.7)
Overall	14937	705 (35.4)	578 (82.0)	374 (64.7)

Clusters 4 and 5 are enriched for differentially expressed genes and TFs. The TFs in these clusters are also enriched for ones that cause wing phenotypes upon misexpression.

Table 3: Comparison of genes with activating and repressive chromatin marks in cluster 4 and 5 with compartmentally expressed genes in the wing disc

Table 3 Many bivalent genes show spatially restricted expression in the wing disc

	Bivalently marked genes / Total number of genes	Bivalently marked genes / Total number of genes
	Cluster 4b	Cluster 5b
All genes	241 / 14940 (1.6%)	194 / 14940 (1.3%)
TF only	70 / 755 (9.3%)	90 / 755 (11.9%)
Genes with A/P or BW/WB restricted expression pattern *		
All genes (427)	35 / 427 (8.2%)	19 / 427 (4.4%)
TF only (54)	27 / 54 (50.0%)	13 / 54 (24.1%)

*** data from (Butler et al., 2003; Ibrahim et al., 2013) and Simigdala (unpublished data)**

References

Adryan, B., and Teichmann, S.A. (2006). FlyTF: a systematic review of site-specific transcription factors in the fruit fly Drosophila melanogaster. Bioinforma. Oxf. Engl. *22*, 1532–1533.

Arnold, C.D., Gerlach, D., Stelzer, C., Boryń, Ł.M., Rath, M., and Stark, A. (2013). Genome-wide quantitative enhancer activity maps identified by STARR-seq. Science *339*, 1074–1077.

Bajpai, R., Chen, D.A., Rada-Iglesias, A., Zhang, J., Xiong, Y., Helms, J., Chang, C.-P., Zhao, Y., Swigut, T., and Wysocka, J. (2010). CHD7 cooperates with PBAF to control multipotent neural crest formation. Nature *463*, 958–962.

Bernstein, B.E., Mikkelsen, T.S., Xie, X., Kamal, M., Huebert, D.J., Cuff, J., Fry, B., Meissner, A., Wernig, M., Plath, K., et al. (2006). A bivalent chromatin structure marks key developmental genes in embryonic stem cells. Cell *125*, 315–326.

Biggin, M.D. (2011). Animal transcription networks as highly connected, quantitative continua. Dev. Cell *21*, 611–626.

Bischof, J., Maeda, R.K., Hediger, M., Karch, F., and Basler, K. (2007). An optimized transgenesis system for Drosophila using germ-line-specific phiC31 integrases. Proc. Natl. Acad. Sci. U. S. A. *104*, 3312–3317.

Bischof, J., Björklund, M., Furger, E., Schertel, C., Taipale, J., and Basler, K. (2013). A versatile platform for creating a comprehensive UAS-ORFeome library in Drosophila. Dev. Camb. Engl. *140*, 2434–2442.

Björklund, M., Taipale, M., Varjosalo, M., Saharinen, J., Lahdenperä, J., and Taipale, J. (2006). Identification of pathways regulating cell size and cell-cycle progression by RNAi. Nature *439*, 1009–1013.

Bonn, S., Zinzen, R.P., Girardot, C., Gustafson, E.H., Perez-Gonzalez, A., Delhomme, N., Ghavi-Helm, Y., Wilczyński, B., Riddell, A., and Furlong, E.E.M. (2012). Tissue-specific analysis of chromatin state identifies temporal signatures of enhancer activity during embryonic development. Nat. Genet. *44*, 148–156.

Brand, A.H., and Perrimon, N. (1993). Targeted gene expression as a means of altering cell fates and generating dominant phenotypes. Dev. Camb. Engl. *118*, 401–415.

Butler, M.J., Jacobsen, T.L., Cain, D.M., Jarman, M.G., Hubank, M., Whittle, J.R.S., Phillips, R., and Simcox, A. (2003). Discovery of genes with highly restricted expression patterns in the Drosophila wing disc using DNA oligonucleotide microarrays. Dev. Camb. Engl. *130*, 659–670.

Cao, R., Wang, L., Wang, H., Xia, L., Erdjument-Bromage, H., Tempst, P., Jones, R.S., and Zhang, Y. (2002). Role of histone H3 lysine 27 methylation in Polycomb-group silencing. Science *298*, 1039–1043.

Capdevila, J., and Guerrero, I. (1994). Targeted expression of the signaling molecule decapentaplegic induces pattern duplications and growth alterations in Drosophila wings. EMBO J. *13*, 4459–4468.

Czermin, B., Melfi, R., McCabe, D., Seitz, V., Imhof, A., and Pirrotta, V. (2002). Drosophila enhancer of Zeste/ESC complexes have a histone H3 methyltransferase activity that marks chromosomal Polycomb sites. Cell *111*, 185–196.

Davidson, E.H. (2006). The Regulatory Genome: Gene Regulatory Networks In Development And Evolution (Burlington, MA□; San Diego: Academic Press).

Davidson, E.H., and Levine, M.S. (2008). Properties of developmental gene regulatory networks. Proc. Natl. Acad. Sci. U. S. A. *105*, 20063–20066.

Deplancke, B. (2009). Experimental advances in the characterization of metazoan gene regulatory networks. Brief. Funct. Genomic. Proteomic. *8*, 12–27.

Dietzl, G., Chen, D., Schnorrer, F., Su, K.-C., Barinova, Y., Fellner, M., Gasser, B., Kinsey, K., Oppel, S., Scheiblauer, S., et al. (2007). A genome-wide transgenic RNAi library for conditional gene inactivation in Drosophila. Nature *448*, 151–156.

Fang, M., Li, J., Blauwkamp, T., Bhambhani, C., Campbell, N., and Cadigan, K.M. (2006). C-terminal-binding protein directly activates and represses Wnt transcriptional targets in Drosophila. EMBO J. *25*, 2735–2745.

Filion, G.J., van Bemmel, J.G., Braunschweig, U., Talhout, W., Kind, J., Ward, L.D., Brugman, W., de Castro, I.J., Kerkhoven, R.M., Bussemaker, H.J., et al. (2010). Systematic protein location mapping reveals five principal chromatin types in Drosophila cells. Cell *143*, 212–224.

Hammonds, A.S., Bristow, C.A., Fisher, W.W., Weiszmann, R., Wu, S., Hartenstein, V., Kellis, M., Yu, B., Frise, E., and Celniker, S.E. (2013). Spatial expression of transcription factors in Drosophila embryonic organ development. Genome Biol. *14*, R140.

Heinz, S., Benner, C., Spann, N., Bertolino, E., Lin, Y.C., Laslo, P., Cheng, J.X., Murre, C., Singh, H., and Glass, C.K. (2010). Simple combinations of lineage-determining transcription factors prime cis-regulatory elements required for macrophage and B cell identities. Mol. Cell *38*, 576–589.

Hens, K., Feuz, J.-D., Isakova, A., Iagovitina, A., Massouras, A., Bryois, J., Callaerts, P., Celniker, S.E., and Deplancke, B. (2011). Automated protein-DNA interaction screening of Drosophila regulatory elements. Nat. Methods *8*, 1065–1070.

Ibrahim, D.M., Biehs, B., Kornberg, T.B., and Klebes, A. (2013). Microarray comparison of anterior and posterior Drosophila wing imaginal disc cells identifies novel wing genes. G3 Bethesda Md *3*, 1353–1362.

Janssen, S., Cuvier, O., Müller, M., and Laemmli, U.K. (2000). Specific gain- and loss-of-function phenotypes induced by satellite-specific DNA-binding drugs fed to Drosophila melanogaster. Mol. Cell *6*, 1013–1024.

Kharchenko, P.V., Alekseyenko, A.A., Schwartz, Y.B., Minoda, A., Riddle, N.C., Ernst, J., Sabo, P.J., Larschan, E., Gorchakov, A.A., Gu, T., et al. (2011). Comprehensive analysis of the chromatin landscape in Drosophila melanogaster. Nature *471*, 480–485.

Langmead, B., and Salzberg, S.L. (2012). Fast gapped-read alignment with Bowtie 2. Nat. Methods *9*, 357–359.

Lunde, K., Biehs, B., Nauber, U., and Bier, E. (1998). The knirps and knirps-related genes organize development of the second wing vein in Drosophila. Dev. Camb. Engl. *125*, 4145–4154.

Marquez, R.M., Singer, M.A., Takaesu, N.T., Waldrip, W.R., Kraytsberg, Y., and Newfeld, S.J. (2001). Transgenic analysis of the Smad family of TGF-beta signal transducers in Drosophila melanogaster suggests new roles and new interactions between family members. Genetics *157*, 1639–1648.

Marty, F., Rockel-Bauer, C., Simigdala, N., Brunner, E., and Basler, K. (2014). Large-scale imaginal disc sorting: A protocol for “omics”-approaches. Methods San Diego Calif.

Matova, N., and Anderson, K.V. (2006). Rel/NF-kappaB double mutants reveal that cellular immunity is central to Drosophila host defense. Proc. Natl. Acad. Sci. U. S. A. *103*, 16424–16429.

McKay, D.J., and Lieb, J.D. (2013). A common set of DNA regulatory elements shapes Drosophila appendages. Dev. Cell *27*, 306–318.

Meyer, S.N., Amoyel, M., Bergantiños, C., de la Cova, C., Schertel, C., Basler, K., and Johnston, L.A. (2014). An ancient defense system eliminates unfit cells from developing tissues during cell competition. Science *346*, 1258236.

Miklos, G.L., and Rubin, G.M. (1996). The role of the genome project in determining gene function: insights from model organisms. Cell *86*, 521–529.

Molnar, C., Casado, M., López-Varea, A., Cruz, C., and de Celis, J.F. (2012). Genetic annotation of gain-of-function screens using RNA interference and in situ hybridization of candidate genes in the Drosophila wing. Genetics *192*, 741–752.

Muse, G.W., Gilchrist, D.A., Nechaev, S., Shah, R., Parker, J.S., Grissom, S.F., Zeitlinger, J., and Adelman, K. (2007). RNA polymerase is poised for activation across the genome. Nat. Genet. *39*, 1507–1511.

Nègre, N., Brown, C.D., Ma, L., Bristow, C.A., Miller, S.W., Wagner, U., Kheradpour, P., Eaton, M.L., Loriaux, P., Sealfon, R., et al. (2011). A cis-regulatory map of the Drosophila genome. Nature *471*, 527–531.

Neumann, C.J., and Cohen, S.M. (1996). Distinct mitogenic and cell fate specification functions of wingless in different regions of the wing. Dev. Camb. Engl. *122*, 1781–1789.

Posadas, D.M., and Carthew, R.W. (2014). MicroRNAs and their roles in developmental canalization. Curr. Opin. Genet. Dev. *27C*, 1–6.

Prelich, G. (2012). Gene Overexpression: Uses, Mechanisms, and Interpretation. Genetics *190*, 841–854.

R Development Core Team. R: A Language and Environment for Statistical Computing. R Foundation for Statistical Computing, Vienna (2014)

Schertel, C., Rutishauser, T., Förstemann, K., and Basler, K. (2012). Functional Characterization of Drosophila microRNAs by a Novel in vivo Library. Genetics.

Schertel, C., Huang, D., Björklund, M., Bischof, J., Yin, D., Li, R., Wu, Y., Zeng, R., Wu, J., Taipale, J., et al. (2013). Systematic screening of a Drosophila ORF library in vivo uncovers Wnt/Wg pathway components. Dev. Cell *25*, 207–219.

Schmitges, F.W., Prusty, A.B., Faty, M., Stützer, A., Lingaraju, G.M., Aiwazian, J., Sack, R., Hess, D., Li, L., Zhou, S., et al. (2011). Histone methylation by PRC2 is inhibited by active chromatin marks. Mol. Cell *42*, 330–341.

Schneider, I. (1972). Cell lines derived from late embryonic stages of Drosophila melanogaster. J. Embryol. Exp. Morphol. *27*, 353–365.

Selbach, M., Schwanhäusser, B., Thierfelder, N., Fang, Z., Khanin, R., and Rajewsky, N. (2008). Widespread changes in protein synthesis induced by microRNAs. Nature *455*, 58–63.

Shin, H., Liu, T., Manrai, A.K., and Liu, X.S. (2009). CEAS: cis-regulatory element annotation system. Bioinforma. Oxf. Engl. *25*, 2605–2606.

Shlyueva, D., Stampfel, G., and Stark, A. (2014). Transcriptional enhancers: from properties to genome-wide predictions. Nat. Rev. Genet. *15*, 272–286.

Simicevic, J., Schmid, A.W., Gilardoni, P.A., Zoller, B., Raghav, S.K., Krier, I., Gubelmann, C., Lisacek, F., Naef, F., Moniatte, M., et al. (2013). Absolute quantification of transcription factors during cellular differentiation using multiplexed targeted proteomics. Nat. Methods *10*, 570–576.

The modENCODE Consortium, Roy, S., Ernst, J., Kharchenko, P.V., Kheradpour, P., Negre, N., Eaton, M.L., Landolin, J.M., Bristow, C.A., Ma, L., et al. (2010). Identification of functional elements and regulatory circuits by Drosophila modENCODE. Science *330*, 1787–1797.

Tupler, R., Perini, G., and Green, M.R. (2001). Expressing the human genome. Nature *409*, 832–833.

Voigt, P., LeRoy, G., Drury, W.J., 3rd, Zee, B.M., Son, J., Beck, D.B., Young, N.L., Garcia, B.A., and Reinberg, D. (2012). Asymmetrically modified nucleosomes. Cell *151*, 181–193.

Voigt, P., Tee, W.-W., and Reinberg, D. (2013). A double take on bivalent promoters. Genes Dev. *27*, 1318–1338.

Weinmann, A.S., and Farnham, P.J. (2002). Identification of unknown target genes of human transcription factors using chromatin immunoprecipitation. Methods San Diego Calif *26*, 37–47.

Ye, T., Krebs, A.R., Choukrallah, M.-A., Keime, C., Plewniak, F., Davidson, I., and Tora, L. (2011). seqMINER: an integrated ChIP-seq data interpretation platform. Nucleic Acids Res. *39*, e35.

Zeitlinger, J., Stark, A., Kellis, M., Hong, J.-W., Nechaev, S., Adelman, K., Levine, M., and Young, R.A. (2007). RNA polymerase stalling at developmental control genes in the Drosophila melanogaster embryo. Nat. Genet. *39*, 1512–1516.

Zentner, G.E., Tesar, P.J., and Scacheri, P.C. (2011). Epigenetic signatures distinguish multiple classes of enhancers with distinct cellular functions. Genome Res. *21*, 1273–1283.

Figure 1

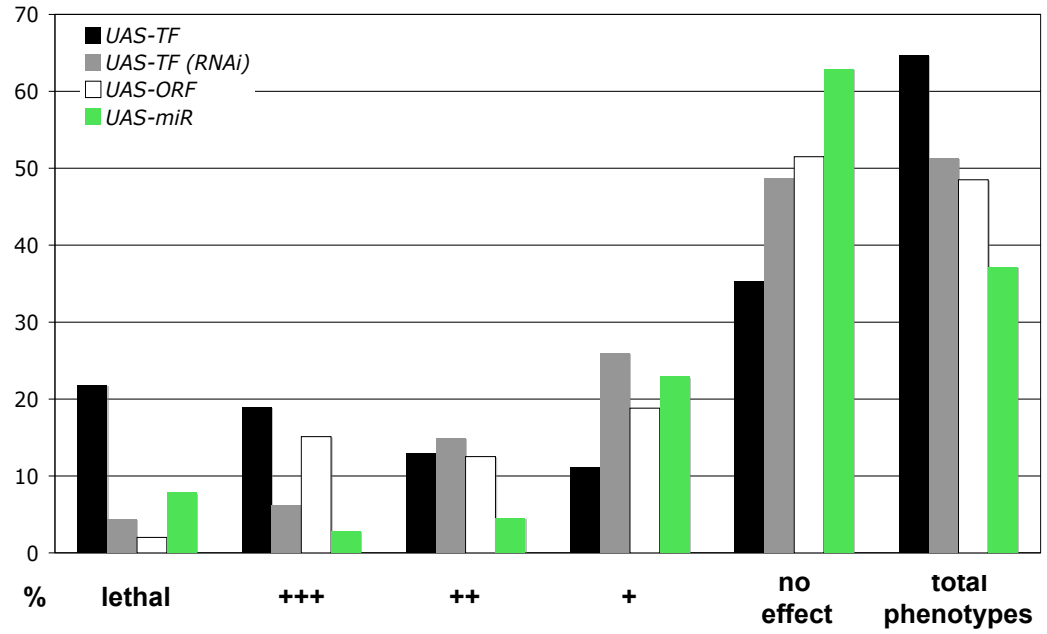
70
60
50
40
30
20
10
0
UAS-TF
UAS-TF (RNAi)
UAS-ORF
UAS-miR
%
lethal
+++
++
+
no effect
total phenotypes


+++
++
+
no effect

Figure 2

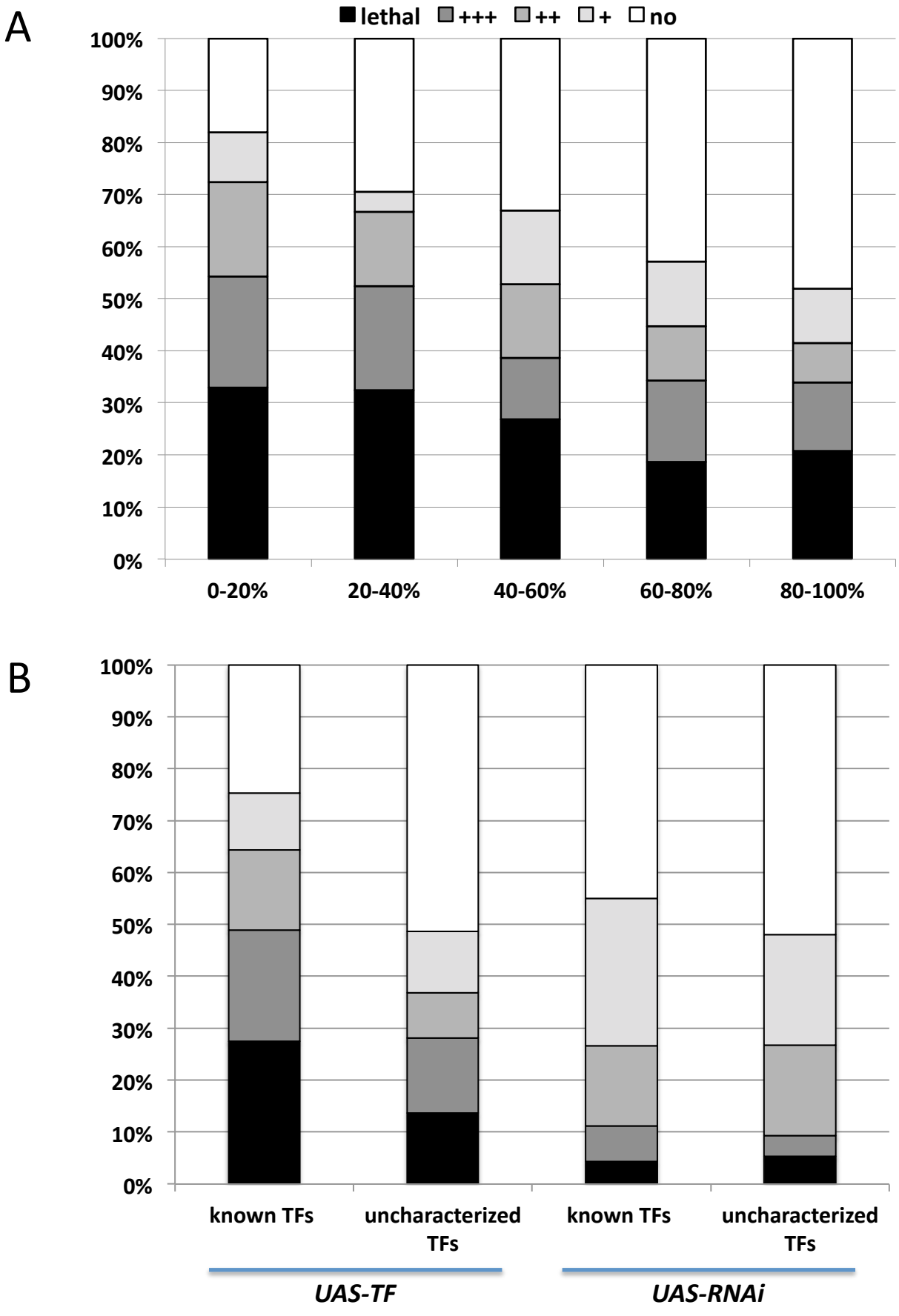
A
lethal
+++
++
+
no
100%
90%
80%
70%
60%
50%
40%
30%
20%
10%
0%
0-20%
20-40%
40-60%
60-80%
80-100%
B
100%
90%
80%
70%
60%
50%
40%
30%
20%
10%
0%
known TFs
uncharacterized TFs
known TFs
uncharacterized TFs
UAS-TF
UAS-RNAi

Figure 3

A

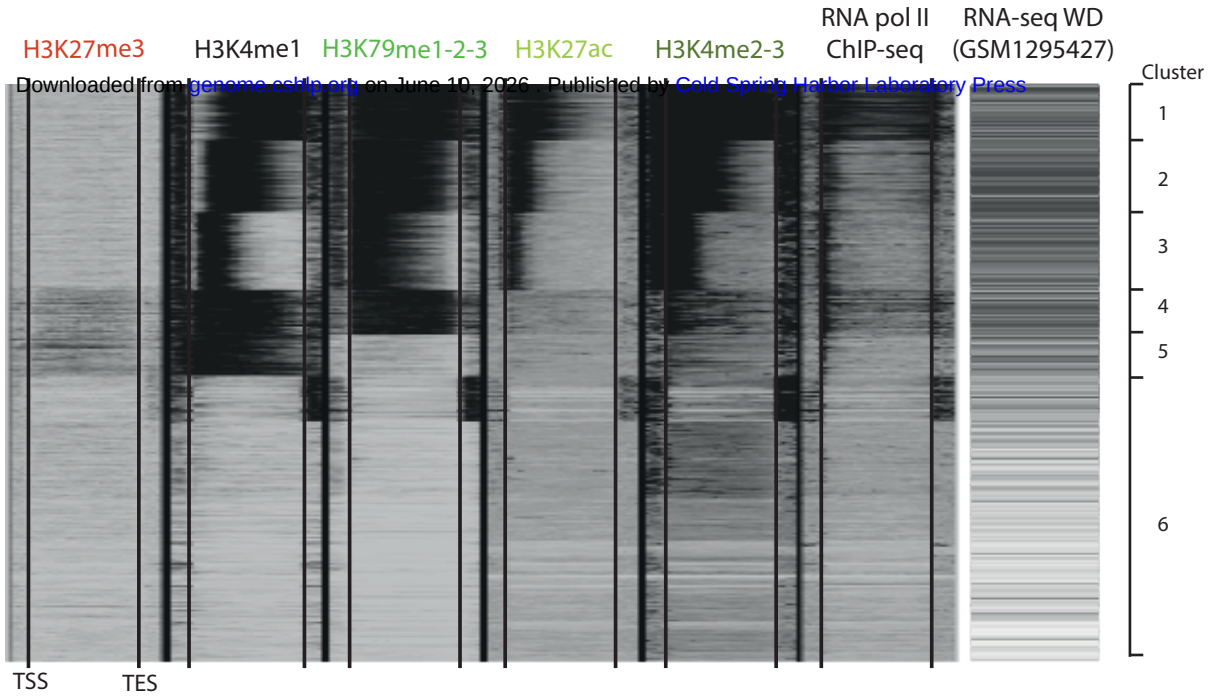

B

Figure 4